Optimizing cross-linking to study the interactions between AQP0 and CaM and AQP2 and LIP5

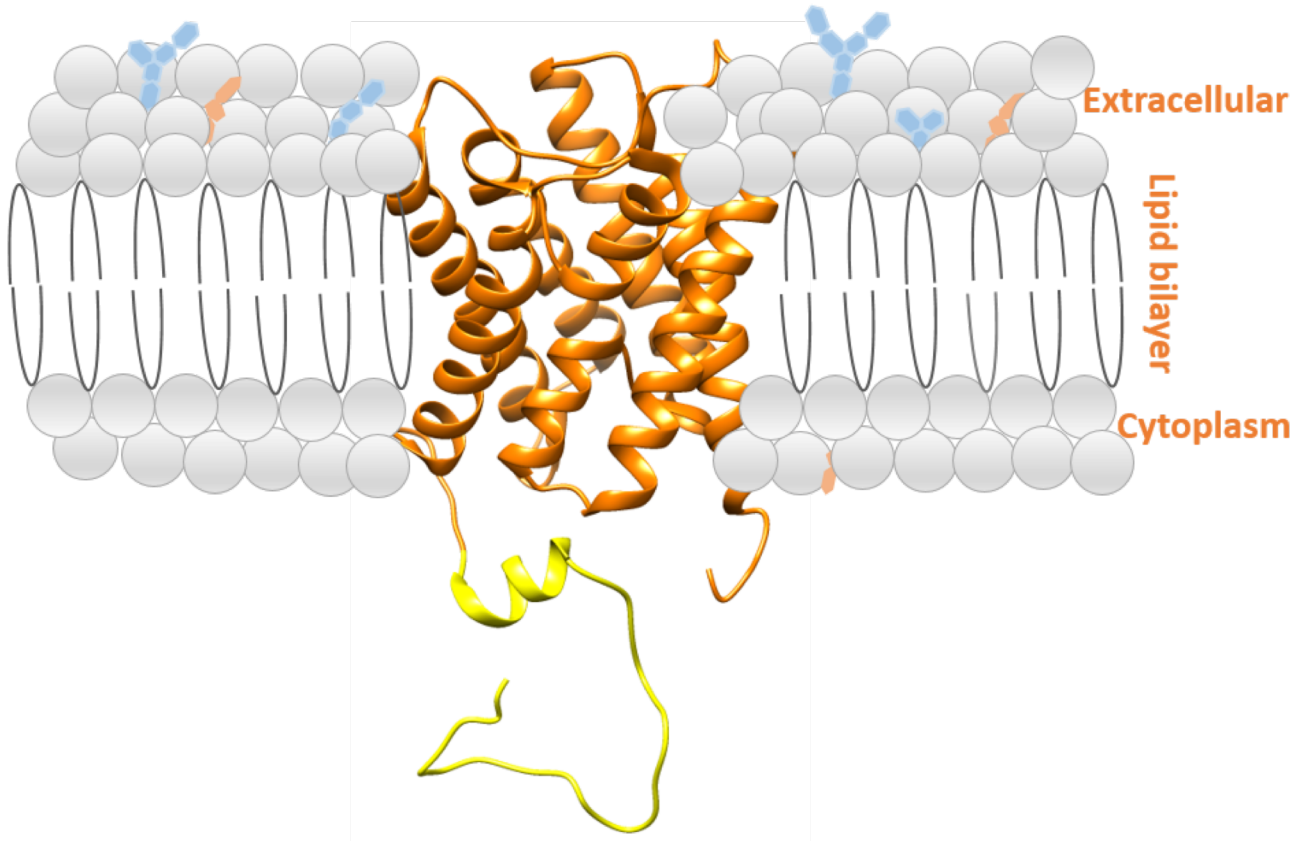

Rawya Antar Hussein
BIOCHEMISTRY AND STRUCTURE BIOLOGY | LUND UNIVERSITY

Optimizing cross-linking to study the interactions between AQP0 and CaM and AQP2 and LIP5

LUNDS UNIVERSITET

Author: Rawya Antar Hussein

Supervisor: Susanna Törnroth-Horsefield

Co-supervisor: Veronika Nesverova

Examiner: Cecilia Emauelsson

Master degree in biochemistry and structural biology

Examensarbete i biokemi 60 hp till masterexamen 2018

Faculty science Lund university

Table of Contents

Popular Science

The faulty interaction between integral membrane protein and regulatory proteins can lead to several diseases. Therefore, studies of these interactions help us understand and answer essential questions on the development and outcome of these disease states. In this project, we investigated two water channels, aquaporin 0 (AQP0) and aquaporin 2 (AQP2) and how they are regulated by calmodulin (CaM) and lysosomal trafficking regulator interacting protein-5 (LIP5), respectively. The aim was to structurally characterize the complexes of these proteins. To reach this aim, AQP0, AQP2, LIP5 and CaM were produced and their ability for interaction was tested using chemical cross-linking and crystallization. The results suggest cross-linking can be used to stabilize the complexes of AQP0 and CaM and AQP2 and LIP5. Furthermore, small crystals were obtained of the complex between the AQP0 C-terminus and CaM.

Abstract

Mammals express thirteen different isoforms of the membrane-bound water channel aquaporin in a tissue-dependent manner. From a medical point of view, two of the most studied isoforms are aquaporin (AQP0), also known as major intrinsic protein and aquaporin 2 (AQP2). AQP0 is exclusively expressed in the mammalian eye lens and responsible for the transport of water across lens fiber cell membranes to maintain lens clarity. The water transport via AQP0 is modulated by CaM, a small protein composed of N and C- terminal calcium (Ca^{2+}) binding domains that connected by an internal flexible linker. AQP2 is expressed in the kidney collecting duct, where it plays a critical role in water reabsorption from urine. AQP2 apical membrane abundance is regulated by trafficking in response to vasopressin, in a phosphorylation-dependent manner. Part of this process involves interacting with lysosomal trafficking regulator interacting protein-5 (LIP5), a small cytosolic protein with a molecular weight of 42 kDa. This interaction, which has been shown to be dependent on AQP2 phosphorylation, facilitates AQP2 lysosomal degradation and therefore balance the abundance of AQP2 in the body. In this project, the main purpose was to develop methods for chemical cross-linking of the AQP0-CaM and AQP2-LIP5 complexes in order to study the structural details of how human aquaporin's interact with regulatory proteins. For this purpose, human AQP0, AQP2, LIP5 and CaM were overproduced and purified, and cross-linking experiments was set up using two different cross-linkers. For both complexes, successful cross-linking could be verified using Western blot. In addition, co-crystallization attempts of the AQP0 C-terminal peptide and CaM was explored, resulting in small crystals that will be further investigated.

1.Introduction

AQPs

Water channels also known as Aquaporin's, are integral membrane proteins that belong to a large family of major intrinsic proteins. Mainly, aquaporin's play a critical role in facilitating transport of water between cells by forming pores in the membrane of biological cells [1]. Water transport mechanism occurs in response to the osmotic gradient [2]. AQPs are highly selective for transferring H_2O and some of them transport a small solute like glycerol [3]. Previous studies such as molecular dynamics simulations observed the mechanism for the selectivity of AQPs to water, which is due to steric factors and electrostatic interaction in the aqueous pore [4]. Malfunction of AQP causes a number of human disease like nephrogenic diabetes insipidus resulting from a loss the function of AQP2, a water channel expressed in the kidney collecting duct. Also mutation or malfunction in AQP0 known as a major intrinsic protein of lens fiber cells is found to be associated with congenital cataracts [5]. However, the mechanism of cataracts results from the reduction of a channel water permeability is still unknown. Mammalian AQPs has thirteen isoforms namely (AQP0-AQP12) that spread out in different cells tissue [6]. Structurally, AQPs monomers assemble as a tetramer in the membrane in which each monomer performs a function pore [7] [8]. A comparison of each AQPs amino acid sequence and structure analysis revealed that each monomer of AQPs consists of six membrane-spanning alpha helices with N and C terminal faced toward the cytosol with two short helical surrounds cytoplasmic and extracellular vestibules that connected by a narrow aqueous pore (Figure 1) [9]. The N- and C- termini and intracellular regions of these isoforms are different [10]. Numerous studies show that these regions are important for the regulation of water transport permeability [11]. Understanding the regulation mechanism is currently the most interesting area for a researcher and two of such mechanisms are the regulation of AQP0 through binding of calmodulin (CaM) to their C- termini in presence of calcium and regulation of AQP2 by LIP5.

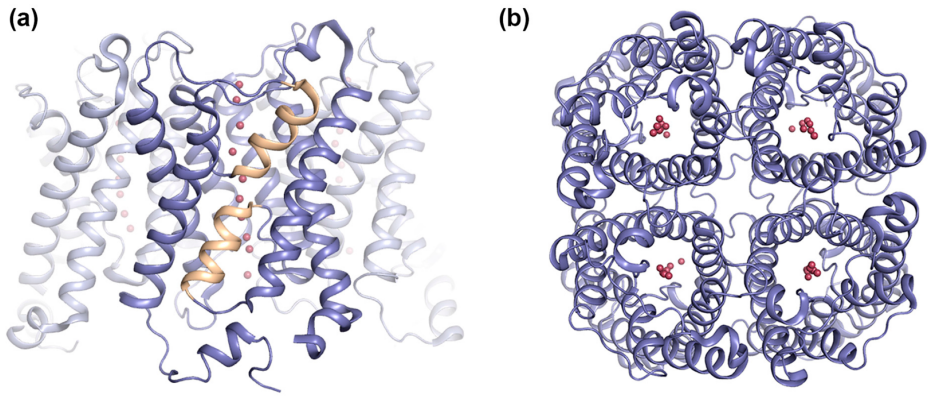

Figure 1: A tetramer of human aquaporin 5 crystal structure (Protein Data Bank 3D9S) [12]. (a) presenting the parallel orientation of tetramer to the membrane with one monomer colored with blue and half-membrane spanning helices colored by yellow. **(b)** shows top view of extracellular face of an AQP5 with water molecules colored in red spherical.

AQP0 membrane protein

AQP0 as previously mentioned is the major intrinsic protein that is expressed in lens fiber cells to perform the transport of water and possibly cell-cell adhesion [11, 13]. The permeability of this channel to transfer the water a cross of the lens is tightly controlled by three mechanisms; acid and alkaline pH sensitivity which is mediated by the externally accessible histidine 66 [14], cleavages of C-termini of AQP0 [15] and Ca^{2+} -calmodulin binding at C-terminus of AQP0 which might be inhibitory or excitatory [16]. In fact, the interaction of FL AQP0 to calmodulin is interesting since the structure of the complex is known, although at low resolution [17].

Calmodulin

Calmodulin is a small protein which consists of 148 amino acids with a molecular weight of 16 kDa [18]. Structurally, CaM is composed of N and C- terminal domain that is connected by an internal flexible linker [19]. Calmodulin is known to bind to calcium ions with high affinity and activated enzyme system in Ca^{2+} -CaM dependent-manner [20]. This protein is found in all eukaryotic cells from yeast to higher mammals and has highly conserved amino acid sequence throughout evolution [21]. CaM binds to calcium at N and C- termini and undergoes dramatic conformational rearrange which results in exposing the hydrophobic binding pocket of CaM as shown in (Figure 2) [22]. The hydrophobic pocket in the CaM binds and regulates numbers of unique target proteins in calcium dependent-manner.

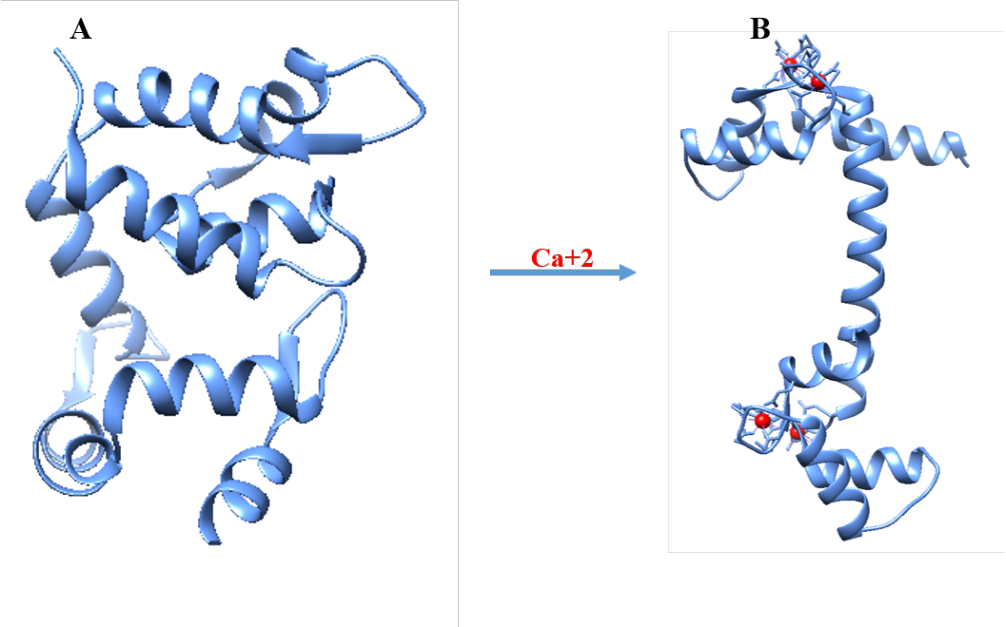

Figure 2: Structure of Calmodulin [23]. A structure of CaM-Ca^{2+} free (PDB 1QX5) colored with cornflower blue. B structure of CaM with four Ca^{2+} ion binding colored with red balls (PDB 1CLL).

Interaction of AQP0 and CaM

Previous studies observed that the AQP0-Ca^{2+} /CaM complex is non-canonical [24]. In addition, the interaction is occurring in which calmodulin interacted simultaneously with two monomers of the C- termini of AQP0 to resulted with 2:1 of CaM: AQP0 tetramer stoichiometry as shown in the (Figure3) [24]. The functional consequence of AQP0- Ca^{2+} - CaM complex formation has been reported to reduce the permeability of the channel with approximately 2-fold [14, 17]. However, the mechanism is poorly understood.

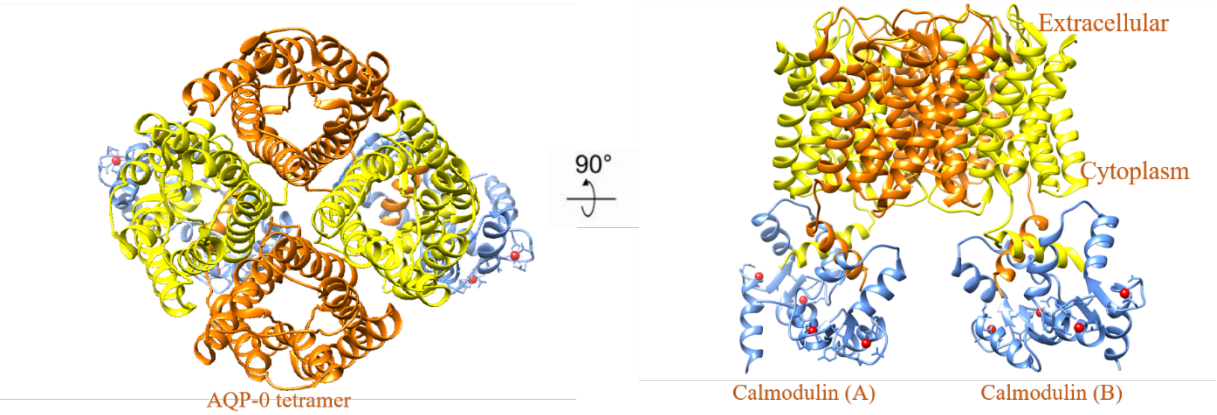

Figure 3: Structure of the AQP0-CaM complex. A tetramer of AQP0 (yellow and orange). interacting with two molecules of CaM (cornflower blue) in presence of Ca^{2+} ion (red balls) [24].

AQP2 membrane protein

Another regulation mechanism that has been extensively studied is the interaction of AQP2 water channel by a lysosomal trafficking regulator interacting protein-5.

AQP2 is the vasopressin-regulated water-channel protein that is expressed in kidney collecting duct, where it plays a critical role in maintaining water homeostasis through the ability to concentrate and dilute urine according to the body hydration state [25]. The location of AQP2 observed to be in apical and subapical of the luminal plasma membrane [26]. Translocation of AQP2, to and from the apical membrane of the renal collecting duct is tightly regulated by the antidiuretic hormone arginine vasopressin (AVP), which is an important factor for water homeostasis [27]. However, many factors have been reported to influence the expression and translocation of AQP2 [28]. Several studies have shown that phosphorylation of the C-terminus of AQP2 is responsible for its apical sorting [29, 30]. In addition, AQP2 abundance is regulated by ubiquitination which occurs through the ubiquitination site at Lys270 [31-33]. Recently, LIP5 is shown to have interactions specifically with the C-terminus of AQP2 and facilitates its lysosomal degradation. Hence, LIP5 is involved in balancing the abundance of AQP2 [27].

LIP5

LIP5 is a cytosolic protein with a molecular weight of 42 kDa. It was reported to be a part of the complex protein machinery that is involved in multivesicular bodies (MVB) [34]. The predominantly function of LIP5 in MVB machinery is to mediated protein for an endosomal compartment that contains many intraluminal vesicles [35]. The luminal vesicles are formed through the invagination of a portion of the limiting membrane and budding into the lumen [36]. However, the structure of full-length LIP5 is unresolved thus making the understanding of the mechanism and interactions with other protein difficult.

LIP5 interaction with C-terminus of AQP2

Degradation of the membrane protein AQP2 occurs after it sorted into the vesicles by budding into MVBs [35]. These MVBs serves as an intermediated station by fusing with either lysosome to deliver the vesicles and their contents for degradation or plasma membrane to release the vesicles as extracellular exosomes. In addition, the formation of MVB vesicles and protein sorting required a different type of proteins, including the Endosomal Sorting Complex Required for Transport (ESCRT) as well as AAA- (ATPase associated with diverse cellular activities) ATPase Vps4. The Vps 4 protein is inducting into the membrane by the complex ESCRT to perform the facility of endosome and formation of the MVB complex [37]. Vsp4

interacts with LIP5 and forms an oligomer ring, which helps the Vsp4 to perform its function in MVB formation [38, 39]. A recent study using far- western blot analysis and microscale thermophoresis (MST) has been shown that AQP2 binds LIP5 in a phosphorylation- dependent manner[40]. However, the mechanism for this complex formation is still unclear and required to be investigated.

The aims of the work

Membrane- protein interactions play an important role in numerous cellular processes. These interactions can be either "transient" occur only to facilitate the signaling or metabolic function or interact "permanently" to forms a multiprotein complex that acts as molecular machines within the living systems. Hence, capturing these binding to study which amino acids are involved and how they interacted becomes the most significant aim for the researcher. In this study, my aim was to characterize the complex of AQP0- CaM and AQP2- LIP5 to study the structural details of how human aquaporin's interact with regulatory proteins. To reach this aim, I optimize protocols of chemical cross-linking. The cross-linked sample will be analyzed by mass spectrometry and crystallization.

2.Experimental procedure

2.1 Production and expression of membrane proteins AQP0 and AQP2

2.1.1 Preparation of Pre-culture of AQP0 and AQP2

To produced full-length human AQP0 and AQP2 in Pichia pastoris, colonies of each were streaked individually on a YPD plate (10 g/L yeast extract, 20 g/L peptone, 20 g/L dextrose and 20 g/L Agar) without antibiotics and growth at 30°C under shaking for overnight. Pre-culture was prepared by suspending a good lump of cells from a plate into 2 × 100 mL of YPD medium (10 g/L yeast extract, 20 g/L peptone, 20 g/L dextrose) in 250 mL flasks. The cells were grown by shaking the flasks in an incubator for overnight at 30° C to have an OD about 25 at 600 nm (OD_{600}) measurement.

2.1.2 Expression of membrane AQP0 and AQP2

Fermentation procedure was performed using Belach bioreactor with two liter working volume, temperature, pH and oxygen modules control. The system was monitored by using HANNA program on a computer. A 100 mL pre-culture from part 2.1.1 was poured into setting up autoclave fermenter containing 1.5 L basal salt medium (40 mL phosphoric acid 85%, 1.395 g calcium sulphate, 27.3 g potassium sulphate, 22.35 g magnesium sulphate*7 H2O, 6.195 g potassium hydroxide, 60 mL glycerol 99.5%). Also, 6.5 mL of particulate trace metals (PTM) and 3 drops of the antifoam were added and the pH was adjusted to 5 by using 25% ammonium hydroxide. The pH was measured, and the temperature was set at 30°C with 25% dissolving oxygen controlled by an electrode with 800 rpm stir speed. Operation of fermenter was monitored in batch mode until all the glycerol in the medium was consumed, which indicated, by a sharp rise in the dissolved oxygen concentration. A feed with 200 mL glycerol (50%) with 2.4 mL of PTM was then started over 6 h with a rate of 15-20 mL/h. The pH was automatically controlled by the electrode to maintain the desired point during glycerol fed-batch phase. After consumption of glycerol, the pump was then switched to feeding with methanol supplied with PTM. The feeding with methanol that serves as inducer and carbon source for recombinant protein expression was continued for two days. The cells were harvested by centrifuging in JLA 8.1000 rotor at 6000 rpm for 30 minutes and stored at -80°C.

2.1.3 Membrane preparation of AQP0 and AQP2

Approximately 50 g of *Pichia pastoris* cells was thawed while stirring in 100 mL of breaking buffer (50 mM potassium phosphate pH 7.5, 5% glycerol and 2 mM Ethylenediaminetetraacetic acid (EDTA)) supplemented with 2mM phenylmethane sulfonyl

fluoride or phenylmethylsulfonyl fluoride (PMSF) and then passed through bead-beating using 200 mL of glass beads for 12 times with 30 sec pulses between each time. The samples were then centrifuged using JLA 10.500 rotor, 9.500 rpm at 4° C for 40 min. The supernatant was transferred into Ti45 tubes and centrifuged using a Ti45 rotor, 45.000 rpm at 4° C for 1 h. After that, the pellet was homogenized using potter homogenizer with urea buffer (5 mM Tris-HCl pH 9.5, 4 M urea, 2 mM EDTA) and centrifuged again as earlier at high speed for 2 h. The supernatant was then discarded and the pellets containing the desired membrane were homogenized using membrane buffer (20 mM Tris-HCl pH8, 20 mM NaCl, 10% glycerol) containing 1 mM PMSF and 2mM EDTA then centrifuged with the Ti45 rotor and 45.000 rpm at 4° C for 1 h15 min. Finally, the pellet was homogenized with 2 mL/ g membrane buffer and flash freezed in liquid nitrogen and saved at -80° C**.**

2.1.4 Solubilisation of membrane AQP0 and AQP2

Membrane suspensions of AQP0 and AQP2 from part 2.1.3 were thawed individually in 25 mL dilution buffer (20 mM Tris-HCl pH 8, 300 mM NaCl, 10% glycerol) supplemented with one tablet free-EDTA (Roche) protease inhibitor at 4° C. Later, 25mL of solubilization buffer (20 mM Tris-HCl pH 8, 300 mM NaCl, 10% glycerol and either 2% n-Dodecyl-β-D-Maltoside (DDM) for solubilizing AQP0 or 4% Octyl Glucose Neopentyl Glycol (OGNG) for solubilizing AQP2) were added drop-wise to the membrane sample and led it solubilize for 30 min at 37° C for AQP0 and 1h at 4° C for AQP2. After solubilizing the membrane sample was centrifuged by Ti70 at 50.000 rpm, for 45 min at 4°C to remove insolubilized material. 20 µL sample was saved for sodium dodecyl sulfate polyacrylamide gel electrophoresis (SDS-PAGE) analysis.

2.2 Production and expression of Calmodulin and LIP5

2.2.1 Pre-culture and Expressions of Calmodulin, LIP5

Pre-culture of full-length human LIP5 with C terminus 6x His-tag and CaM without His-tag were grown individually in 120 mL Luria-Bertani (LB) medium (10 g of Tryptone, 5 g Yeast extract 5 g and 10 g NaCl) supplement with 50 µg/mL of ampicillin at 37° C and shaking overnight at 200 rpm. This pre-culture was inoculated in a 2 L-baffled flask with 500 mL of LB in each supplement with 50 µg/mL of ampicillin at 37° C and 180 rpm. The growth of cells was monitored every 30 min by measuring the OD_{600}. The initial OD was set to approximately 0.05- 0.1. The cells were induced with 0.5 mM IsoPropylThio-β-Galactoside (IPTG) after the

OD_{600} was about 0.8- 1.0 and let it to grow for 4 h. The cells were then harvested by using JLA 10.500 rotor at 6000 rpm for 15 min and stored at -20 °C.

2.2.2 Lysis cells and preparation of Calmodulin and LIP5 for purification

Bacteria pellet containing overexpressed CaM and LIP5 were suspended individually in lysis buffer (50 mM Tris-HCl pH 7.5, 2 mM EDTA and 2 mM PMSF), (20 mM Tris-HCl pH 8, 250 mM NaCl, 5% glycerol 10 mM imidazole supplement with 1 tabled complete EDTA free (Roche). The cells were lysed by sonication with 50% duty cycle and 4 outputs for 1 min X5 and a min rest in between. The suspension was then centrifuged using JA 25.50 rotors at 15000 rpm, 4° C for 30 min. The supernatant was kept until purification.

2.3 Proteins purification

2.3.1 Proteins purification using immobilized metal-affinity chromatography (IMAC)

Soluble membrane protein (approximately 50 mL) from part 2.1.4 and supernatant of LIP5 from part 2.2.2 were purified using BioRad chromatography system and HisTrap™ HP 5 mL column (GE Healthcare Life Science). The column was equilibrated with 5 CV degassed equilibration buffer (Table 1) and the sample was loaded onto the column using a super loop at 1ml/min. The column was washed with degassed wash buffer (Table 1) supplied with 33% of elution buffer. Protein was eluted from the column using elution buffer (Table 1). From each peak on the chromatogram, 20 µL sample was taken for SDS-PAGE analysis. The peak containing the desired protein sample was collected and concentrated to about 500 µL using a VivaSpin 2 (GE Healthcare) as shown (Table 2). His-tag was removed from the C-terminus of LIP5 using 1:100 ratio of Tobacco Etch Virus (TEV) enzyme: LIP5 in presence of 0.5 mM of TCEP as a final concentration for an overnight incubation. The sample was purified on Reverse- phase His-Trap using poly-prep (Bio-rad) column loaded with 1 ml of Ni-NTA free beads using the same buffer as previously described in normal IMAC purification. After purification of AQP0, AQP2 and LIP5, the buffers were exchanged with gel filtration buffer using a VivaSpin 2 column (MWCO 10 kDa) followed by concentrating the sample to approximately 500µL for size exclusion chromatography.

Table 1: A list of buffers used in immobilized metal-affinity chromatography.

Buffer name	Recipe
Equilibration buffer	20 mM Tris-HCl pH 8, 300 mM NaCl, 10% glycerol, 10 mM imidazole and either 0.03% DDM for AQP0 or 0.2% OGNG for AQP2, and (20 mM Tris-HCl pH 8, 250 mM NaCl, with 5% glycerol for LIP5
Washing buffer	(20 mM Tris-HCl pH 8, 300 mM NaCl, 10% glycerol, 75-100mM imidazole and either 0.03% DDM for AQP0 or 0.2% OGNG for AQP2) or (20 mM Tris-HCl pH 8, 250 mM NaCl, with 5% glycerol) for LIP5
Elution buffer	(20 mM Tris-HCl pH 8, 300 mM NaCl, 10% glycerol, 300 mM imidazole and either 0.03% DDM for AQP0 or 0.2% OGNG for AQP2) or (20 mM Tris-HCl pH 8, 250 mM NaCl, with 5% glycerol, 300 mM imidazole for LIP5

2.3.2 Purification of proteins by Size Exclusion Chromatography (SEC)

For high purity proteins, approximately 700 µL concentrated sample from IMAC purification step was loaded on superdex 200 10/300 column (GE Healthcare Life Science) at 4° C. SEC of AQP0, AQP2 and LIP5 were performed in specific buffers mentioned in Table 2. The column was equilibrated with 50 mL degassed buffer and loaded the sample on the column. To elute the protein, the column was washed with 50 mL gel filtration buffer and run at 0.4 mL/min for two CV. After that 20 µL were taken from each sample of peak containing the desired protein for SDS-PAGE analysis. The peak containing the desired protein was collected and concentrated to approximately 500 µL using a VivaSpin 2 as shown (Table 2). The concentration was measured by NanoDrop™ (Thermo Scientific™) UV-Vis spectrophotometers and samples were stored at -80° C for later use in cross-linking reaction.

Table 2: Buffer recipe for size exclusion chromatography.

Protein Name	SEC buffer recipe	VivaSpin 2 column
AQP0	20 mM HEPES pH 7.5, 100 mM NaCl, 5% glycerol, 0.03% DDM and 5 mM CaCl2)	MWCO 50 kDa
AQP2	20 mM Tris-HCl pH 8, 300 mM NaCl, 0,2% OGNPG	MWCO 50 kDa
LIP5	20 mM Tris-HCl pH 8, 150 mM NaCl and 1 mM DTT	MWCO 10 kDa

2.3.3 One step purification of CaM by hydrophobic interaction chromatography

The supernatant of CaM in 2.2.2 containing 5 mM CaCl2 was purified using poly-prep (Bio-rad) column loaded with 1 ml of phenyl sepharose CL-4B free beads. The column was equilibrated with (50 mM Tris-HCl pH 7.5, 0.1 M NaCl, 5 mM CaCl2) buffer and the sample was injected to the column at room temperature. The column was washed with approximately 50 mL of (50 mM Tris-HCl, 0.5 M NaCl, 0.1 mM CaCl2) buffer. The protein eluted from the column using elution buffer (50 mM Tris-HCl, 1 mM EGTA). From each step, a 20 µl samples were taken for SDS-PAGE analysis. The protein was concentred using a VivaSpin 2 (MWCO 3kDa) and the concentration was measured by NanoDrop™ (Thermo Scientific™).

2.4 Standard preparation of Sodium Dodecyl Sulfate PolyacrylAmide Gel Electrophoresis (SDS-PAGE)

Denaturing SDS-PAGE was performed as per the instructions of Invitrogen NuPAGE®. approximately, 20 µL of total lysate, samples from IMAC and samples from GF were mixed individually with 20 µL loading buffer (187.5 mM Tris HCl pH 6.8, 6% (w/v) SDS, 30% (v/v) glycerol 0.03% (w/v) bromphenol blue, 120 mM Dithiothreitol (DTT). 10 µL of each sample was then loaded on precast NuPAGE Novex 4-12% Bis-Tris gels. About 5 µL of spectra multicolour broad range protein ladder (Thermo Scientific) was used as size marker. Electrophoresis was carried out for 35 min at room temperature (RT) using constant voltage (200V) in (50 mM MES, 50 mM Tris-base, 0.1% SDS and 1 mM EDTA) buffer. The SDS-PAGE gel was washed 3X with water and microwaved for 25 seconds in between each wash and then stained using Simple Blue™ Safe Stain (Novex). Followed with destined according to Novex fast stain protocol.

2.5 Complex formation of AQP0-CaM, AQP2-LIP5 and purification

2.5.1 Cross-linking experiment using zero- length EDC- NHS cross-linker

EDC is zero-length heterobifunctional cross-linker. The protocol was done in two steps, according to the manufacturer (Thermo Scientific). The first step also known as (activation reaction) was performed using 3.28 mg/mL of CaM in activation buffer (100 mM MES pH 6, 500 mM NaCl and 5 mM CaCl2), and 1-ethyl-3-[3-dimethylaminopropyl]carbodiimide hydrochloride (EDC) was added to a final concentration of 2 mM. Followed by adding *N*-hydroxysulfosuccinimide (Sulfo-NHS) to a final concentration of 5mM. The reaction was incubated at room temperature for 15 min and 20 µL was taken for SDS-PAGE and Western blot analysis. Then the activation reaction was quenched with 1.4 µL/ml of 20 mM B-MeOH. The crosslinking reaction is the most efficient at pH 7, so the buffer was exchanged to HEPES buffer (20 mM HEPES pH 7.5, 100 mM NaCl 5% glycerol, 0,03% DDM and 5 mM CaCl2) and concentrated to about 500 µL using a VivaSpin 2 (MWCO 50 kDa). The second step was performed by adding 10 mg/ mL of AQP0 to the reaction and incubated at room temperature for 2 h. About 20 µL of cross-linking reaction was taken for SDS-PAGE and Western blot analysis and the rest quenched with 1 M Tris-HCl containing 0.03% DDM at 100 mM final concentration. The same reaction was done for AQP2-LIP5 but in this reaction, AQP2 was activated first with EDC and NHS and buffer was exchanged to phosphate buffer (100 mM calcium phosphate pH 7.4, 150 mM NaCl and 0.25% OGNPG).

2.5.2 Cross-linking experiment using mid-length BS3 cross-linker

Cross-linking experiment was also performed using different cross-linker known as BS3 (bis(sulfosuccinimidyl)suberate) that specifically crosslinks lysine residues. 50 µM of each full-length AQP0 and C-terminus AQP0 were individually mixed with 50 µM of CaM. A stock of 30 mM BS3 was prepared and 1.9 µL BS3 added to the previous protein mixture followed by adding (50 mM HEPES pH 8, 5 mM CaCl2 and 100 mM NaCl) buffer in 20 µL total volume. The reaction was allowed to proceed for 30 min at room temperature followed by quenching the reaction using 30 mM final concentration of 1M Tris- HCl pH 8. Sample volume of 5 µL was taken for SDS-PAGE analysis and the rest was stored at -20° C for later use in mass spectrometry analysis.

2.5.3 Preparation of Western blot

Sample from each step of cross-linking reaction mixed with loading buffer in 1:1 ratio. About 10 µL of this mixture was loaded on the SDS_PAGE gel as described in the standard SDS-PAGE method in 2.4. The gel then transferred to Nitrocellulose blotting membrane (GH Health

Care Life Science) using non-reduced transfer buffer (25 mM Bicine, 25 mM Bis-Tris free base, 1 mM EDTA at pH 7.2). The transfer condition was set to 30 V for 1 h with current started from 170 mA and end with 110 mA. The membrane was then soaked with 20 mL blocking solution of 5% (w/v) milk powder dissolved in TBS-T buffer (20 mM Tris-HCl pH 7.4, 150 mM, NaCl and 0.2% Tween-20) for 15 min. 4 µL of mouse 6XHis-tag for AQP0 or Rabbit 6 XHis-tag for AQP2 (Clontech) primary antibody added to the blocking solution and incubated for 1 h at room temperature. The incubated membrane was washed three times with TBS-T buffer for 15 min between each wash. 20 mL of blocking solution was added to the membrane and incubated for 15 min and 4 µL of an anti-mouse antibody or anti-Rabbit (Clontech) added to the membrane and incubated for 1 h at RT. The incubated membrane was washed three times with TBS-T buffer for 15 min between each wash.

Detection of transferred gel to the membrane was done using ELC™ Prime Western blotting detection reagent where equal volumes (500 µL) of each Prime Luminal Enhancer Solution A and Prime peroxide solution B were mixed. The reagent was added on the membrane and left for 2 second. After that, the signal was detected using SYNGENE PXi machine.

2.5.4 Purification of complex AQP0-CaM by anion exchange chromatography

Cross-linked complex of AQP- CaM was purified in Resource Q 6mL column (GE Healthcare Life Science). The column was equilibrated with equilibration buffer (20 mM Tris- HCl pH 8, 100 mM NaCl, 5% glycerol, 0.03% DDM and 5 mM CaCl2) and then the sample complex of AQP0-CaM loaded on the column using 2 mL/ min flow rate at 4° C. The column was washed with 5CV with equilibration buffer and the complex was eluted by elution buffer (20 mM Tris-HCl pH 8, 5% glycerol, 0.03% DDM, 5 mM CaCl2 and 1000 mM NaCl). A 20 µl sample of each peak on chromatogram was taken for SDS_PAGE and Western blot analysis.

2.6 Crystallization

To set up crystals, about 10 mg/mL AQP0 C-terminal peptide (GenScript) was mixed with 10 mg/mL of CaM from part 2.3.3 at three different molar ratios (2:1, 3:1 and 4:1) of AQP0: CaM. The sitting-drop crystal screens were set-up using PACT premier and JCSG- plus screen at 20° C at crystallization facility (Lund University) using the Mosquito robot. The drop size was 100 nL of protein plus 100 nL of precipitant solution.

3. Results

3.1 Expression and purification of AQP0, AQP2, LIP5 and CaM

In this study, full-length human AQP0 and AQP2 containing a C-terminal 6xHis-tag and N-terminal 8xHis-tag respectively were produced in *Pichia-pastoris*, Table 3. In addition, human LIP5 with a C-terminal 6xHis-tag and human CaM without a tag were produced in *E. coli*, Table 3. Subsequently, each protein was purified using IMAC and SEC except CaM, which was purified using hydrophobic interaction chromatography. Figure 4 shows the purification of AQP0 using SDS-PAGE as well as chromatograms of elution profile from His-Trap and SEC. The SDS-PAGE gels and His-Trap, SEC chromatograms of purifying AQP2, LIP5 and SDS-PAGE of hydrophobic interaction chromatography of CaM purification are as shown below (Figure 5, 6 and 7).

Table 3: Yield and molecular weight of proteins during expression and purification.

Protein name	Molecular weight (kDa)	Cells	Membranes (per g of cells)	Pure protein (per g of membranes or cells)
AQP0	29	850 g per 1,5 L	8 g (per 90 g of cells)	4 mg/ 6 g of membranes
AQP2	28	700 g per 1,5 L	12 g (per 90 g of cells)	4 mg/ 4 g of membranes
LIP5	42	12 g per 2 L	-	1.25 mg/ 8 g of cells
CaM	16	8 g per 2 L	-	0.6 mg/ 8 g of cells

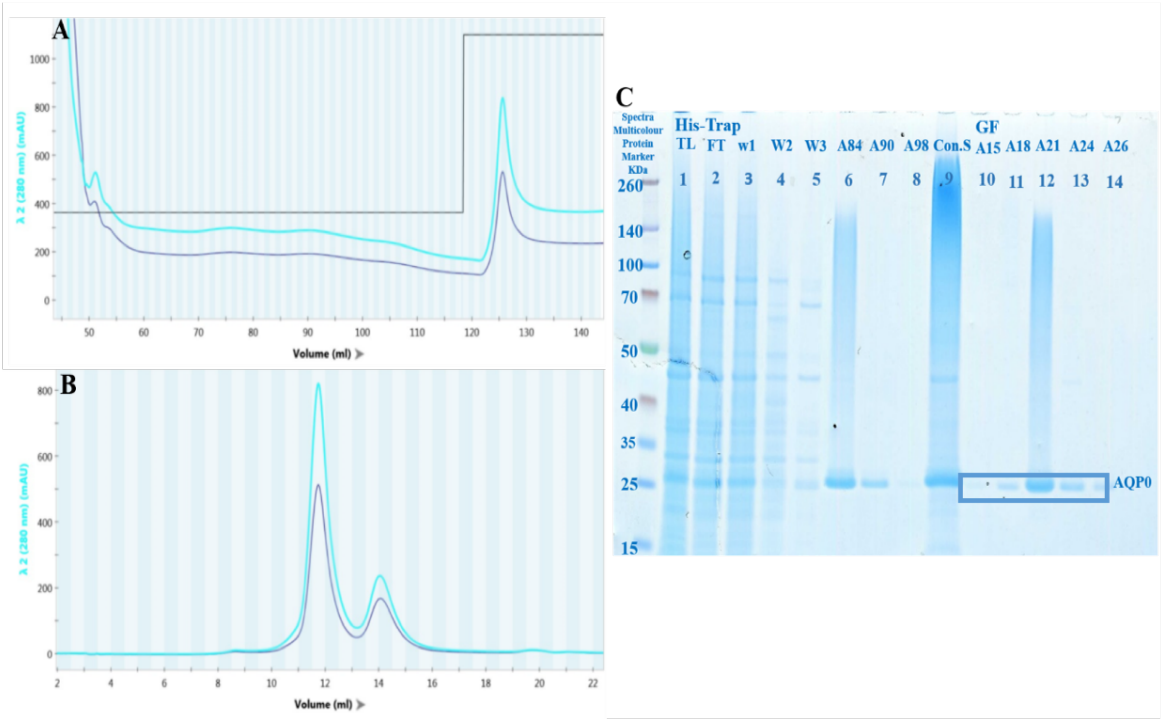

Figure 4: Two-step purification of AQP0 on IMAC and SEC. (A) the elution profile of AQP0 using His-trap, **(B)** the elution profile of AQP0 using SEC and **(C)** SDS-PAGE gel; lane 1 and 2 represent total lysate (TL), flow-through (FT), respectively. Lane 3, 4 and 5 show the washing sample (W1, W2 and W3) during wash the column. Lane 6, 7 and 8 correspond to selected elution fractions (A84, A90 and A98) from first step purification IMAC column. Lane 9 represents the pool of selected and concentrated sample (Con.S) of (A84, A90 and A89) that was loaded on SEC column. Lane 10, 11, 12, 13 and 14 show gel filtration sample (A15-A26) that were collected and concentrated and used for cross-linking reaction (blue rectangle). The first well corresponds to the multicolor protein marker.

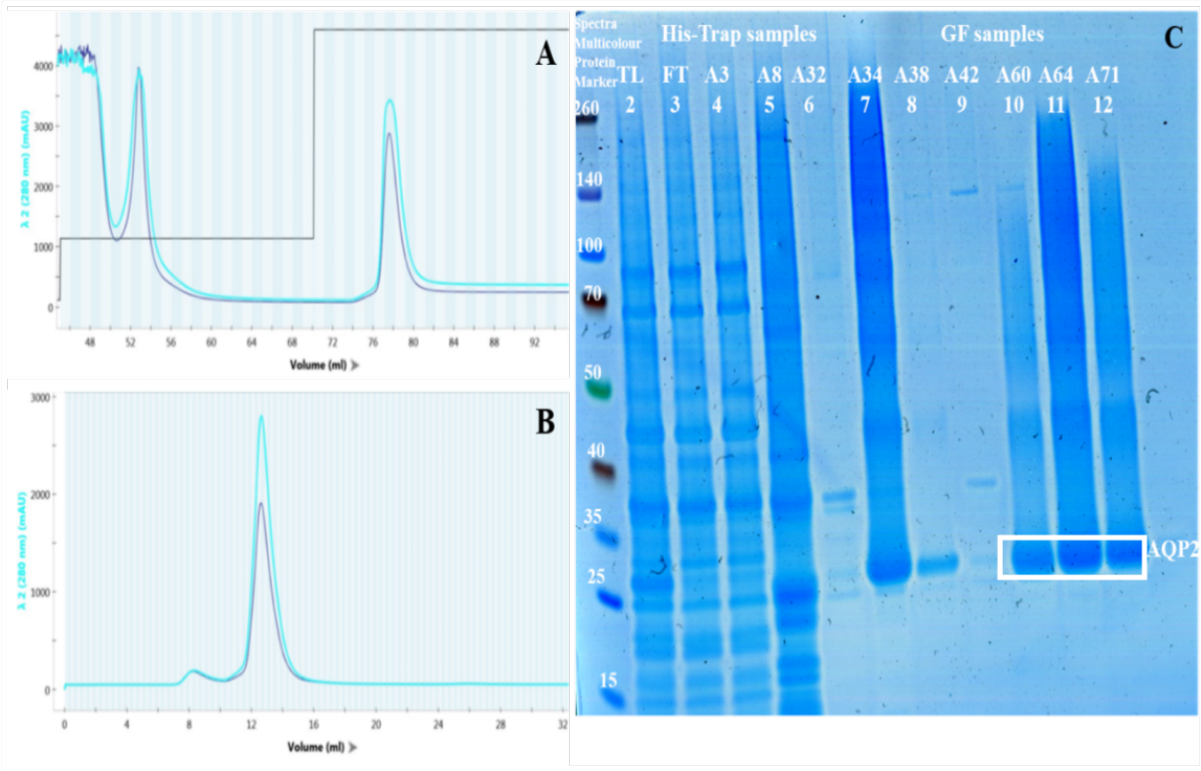

Figure 5: Purification of AQP2 on IMAC and SEC. Elution profile of AQP2 using **(A)** His-trap and **(B)** SEC. **(C)** SDS-PAGE gel; A first lane shows the multicolor protein marker. Lane 2 ,3, 4 and 5 represent total lysate (TL), flow-through (FT) and washing column samples (A3 and A8), respectively. Lane 6,7 and 8 correspond to selected elution fractions (A32, A34 and A38) of the affinity-tagged AQP2 after the first IMAC column that were collected, concentrated and further purified on SEC chromatography. Lane 9 shows fraction (A42) and correspond to the small peak on the chromatograms of SEC profile (**B)** that might be aggregations of AQP2. Lane 10, 11 and 12 correspond to gel filtration sample (A60, A64 and A71) that were collected, concentrated and used for cross-linking reaction, white rectangle.

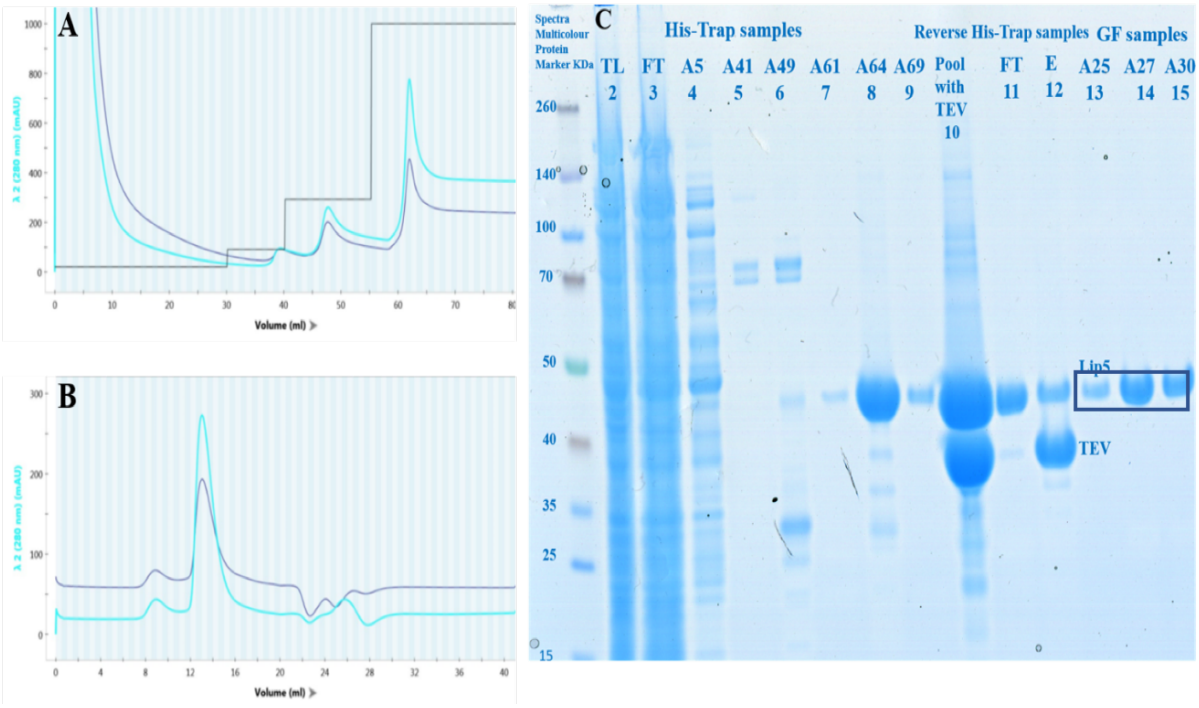

Figure 6: Purification of LIP5 on IMAC, Reveres-His-trap and SEC. (**A**) the elution profile of LIP5 using His-trap, (**B**) the elution profile of LIP5 using SEC and **(C)** SDS-PAGE gel; A first lane corresponds to multicolor protein marker. Lane 2 and 3 represent total lysate (TL) and flow-through (FT), respectively. Lane 4, 5 and 6 show washing samples (A5, A41 and A49) during wash the column. Lane 7, 8 and 9 correspond to elution fractions (A61-A69) from first step purification IMAC column that were collected and treated with TEV- protease. Lane 10 represents the pooled selected fraction (pool with TEV) after overnight treatment. Lane 11 corresponds to flow through (FT) that was collected and further purified on SEC chromatography. Lane 12 shows elution fraction (E) plus TEV after second IMAC column. Lane 13, 14 and 15 show gel filtration sample (A25-A30) that were collected, concentrated and used for cross-linking reaction, blue rectangle.

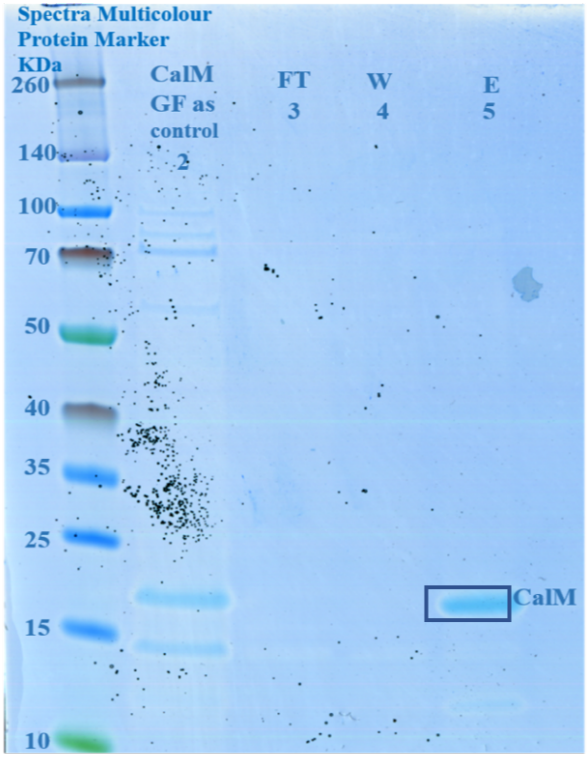

Figure 7: Purification of CaM by hydrophobic interaction chromatography. A first lane represents the multicolor protein marker. Lane 2 shows CaM sample as control. Lane 3 and 4 correspond to flow-through (FT), washing column sample (W), respectively. Lane 5 corresponds to the elution sample (E) of CaM, blue rectangle.

The molecular weight and the yield of AQP0, AQP2, LIP5 and CaM from purification step are presented, Table 3.

3.2 Optimization of the cross-linking reactions for the interactions between AQP0 to CaM and AQP2 to LIP5

Binding between AQP0 to CaM and AQP2 to LIP5 were studied by cross-linking experiment using zero length EDC cross-linker. In order to confirm the formation of the complex, a SDS-PAGE gel and Western blot were performed. For the cross-linking reaction to take place the EDC cross-linker together with sulfo-NHS were used to covalently link the carboxyl group in CaM and AQP2 to amino group in AQP0 and LIP5 with zero-length distance (Figure 8), respectively. The cross-linking reaction was performed in different conditions.

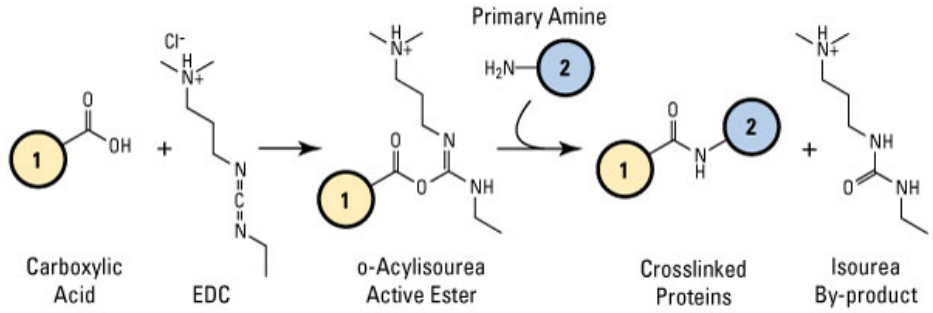

Figure 8: Mechanism of EDC- sulfo- NHS cross-linker.

3.2.1 Cross-linking experiment of AQP0 and CaM

For the formation of the complex of full-length AQP0-CaM, the reaction was first tested at two different molar ratios of the cross-linker 1:10:25 and 1:20:50 of CaM: EDC-NHS with two different pH values, 5.5 and 6.5 as shown in Figure 9 A. The results show that three bands were formed on the gel during activation of CaM that corresponds to monomer, dimer and trimer of CaM cross-linked to itself. In addition, SDS-PAGE demonstrates another three bands during cross-linking reaction with AQP0 that represent CaM, AQP0 and dimer of CaM. These results were further investigated by Western blot using 6X His-tag antibody against N-terminus AQP0, Figure 9 B. Western blot analysis was in agreement with the results of SDS-PAGE gel.

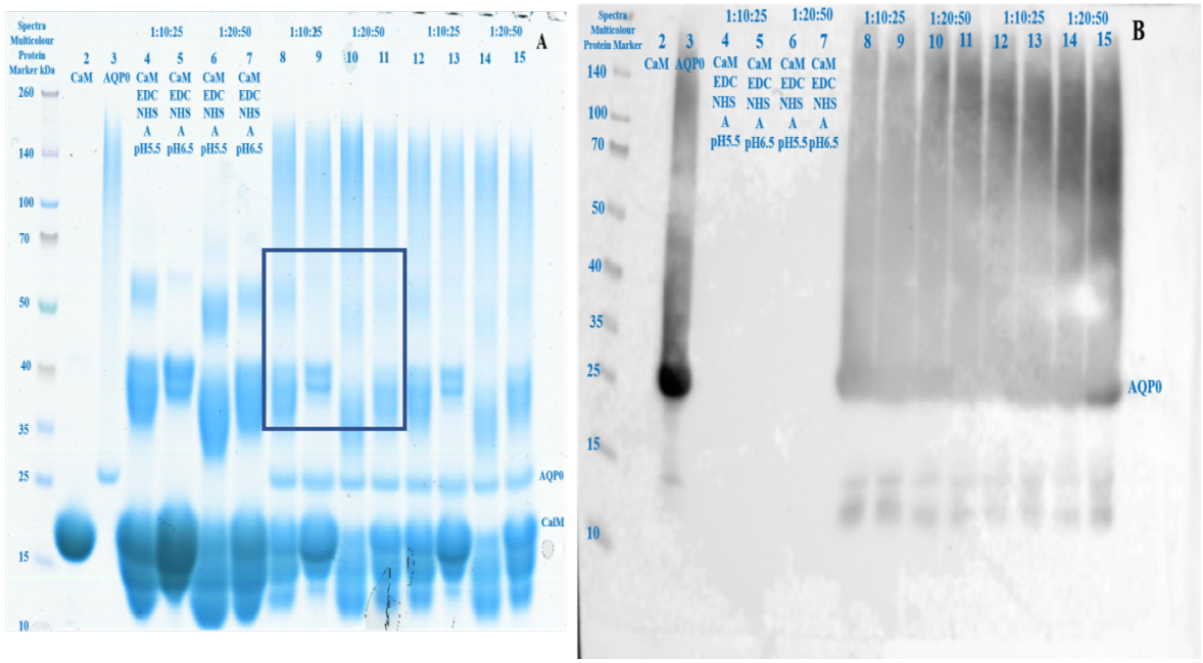

Figure 9: Cross-linking experiment of AQP0. SDS-PAGE **(A)** and Western blot **(B)** for the formation of the complex of AQP0-CaM. The sample order was the same on both gel. The first lane shows the multicolour protein marker. Lane 2 and 3 correspond to the CaM and AQP0, as a control, respectively. Lane 4 and 5 present the CaM activation with EDC and sulfo-NHS at molar ratio 1:10:25 of CaM:EDC: NHS in pH 5.5 and 6.5, respectively. Lane 6 and 7 show the CaM activation with EDC and sulfo-NHS at molar ratio 1:20:50 of CaM: EDC: NHS in pH 5.5 and 6.5, respectively. Lane 8 and 9 present the crosslinking reaction of CaM with AQP0 for 2h (room temperature) at molar ratio 1:10:25 in pH 5.5 and 6.5, respectively. Lane 10 and 11 show the crosslinking reaction of CaM with AQP0 for 2 h (room temperature) at molar ratio 1:20:50 in pH 5.5 and 6.5, respectively. The blue box on SDS-PAGE shows the formation of possible complex of full-length AQP0-CaM that was investigated by Western blot.While lane 12 and 13 correspond to the same cross-linking reaction as in 8 and 9 but incubation was over-night. Also, lane 14 and 15 is the same as cross-linking reaction as in 10 and 11 with incubation over-night.

The cross-linking experiment was repeated using 5 mM of Ca^{2+} ion during activation of CaM and the resulted samples were analyzed using SDS- PAGE gel, Figure 10 A. Again, the gel showed dimer and trimer of CaM during activation of CaM with EDC-NHS cross linker. In addition, the results illustrate a formation of two bands of possible complex together with unreacted AQP0 and CaM. The two bands were approximately around 60 kDa and 40 kDa, which are corresponded to the possible complex of 2:1 and 1:1 of AQP0: CaM, respectively. In order to confirm these results, a Western blot was performed using the 6X His-tag antibody

against the N- terminus AQP0. Figure 10 B shows the formation of these two bands together with band corresponds to AQP0.

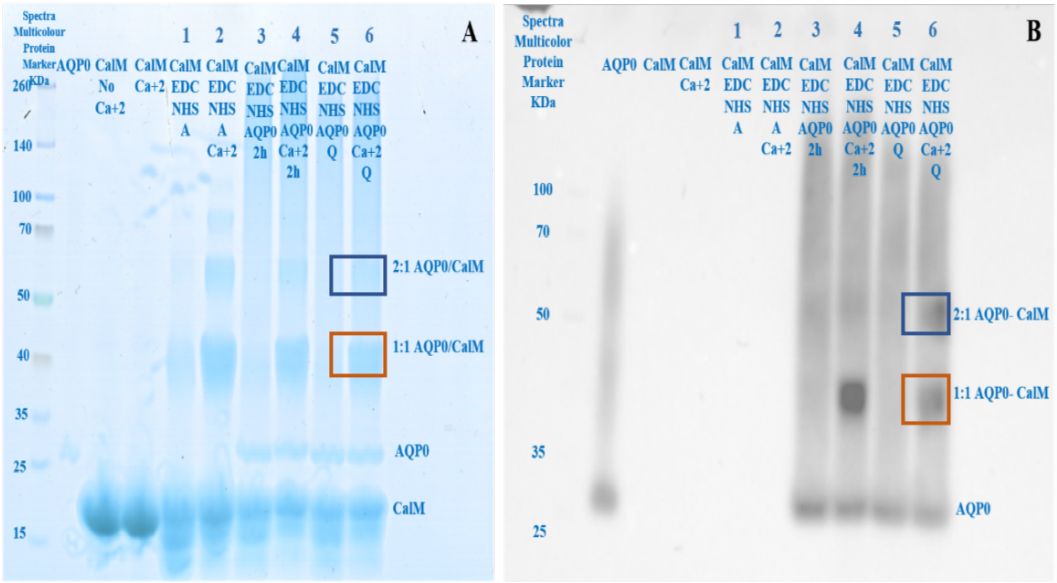

Figure 10: Cross-linking experiment of AQP0 using 5 mM of Ca^{2+} ion during activation of CaM. Samples order on both gel was the same. (**A)** shows the SDS-PAGE gel and (**B)** Presents Western blot; first column corresponds to the multicolor Spectra protein marker. Second, third and fourth column present AQP0, CaM without Ca^{2+} and CaM with Ca^{2+} as control, respectively. Lane 5 and 6 show the CaM activation with EDC and NHS in absences of Ca^{2+} and in presence of Ca^{2+}, respectively. Lane 3 and 4 correspond to incubation of activated CaM with AQP0 for 2 h at room temperature with and with-out Ca^{2+} respectively. Lane 5 and 6 are the same cross-linking reaction as in 3 and 4 but with quenching reaction (stop the cross-linking reaction by adding quenching buffer (1 M Tris-HCl pH 7.5, 0.3% DDM)). Blue and orange boxes show the formation of possible complex of 2:1 and 1:1 of AQP0: CaM, respectively.

The complex in the previous cross-linked experiment was purified on an anion-exchange to remove unreacted AQP0. The elution profile is presented in Figure 11 A. The outcome sample from the anion exchange together with AQP0 and CaM as a positive control and previous cross-linked reaction were analyzed on SDS-PAGE, Figure 11 B. The chromatogram shows a peak at almost 160 mL, which is not observed on SDS-PAGE. This could be due to the accidentally taken the incorrect sample from purification plate.

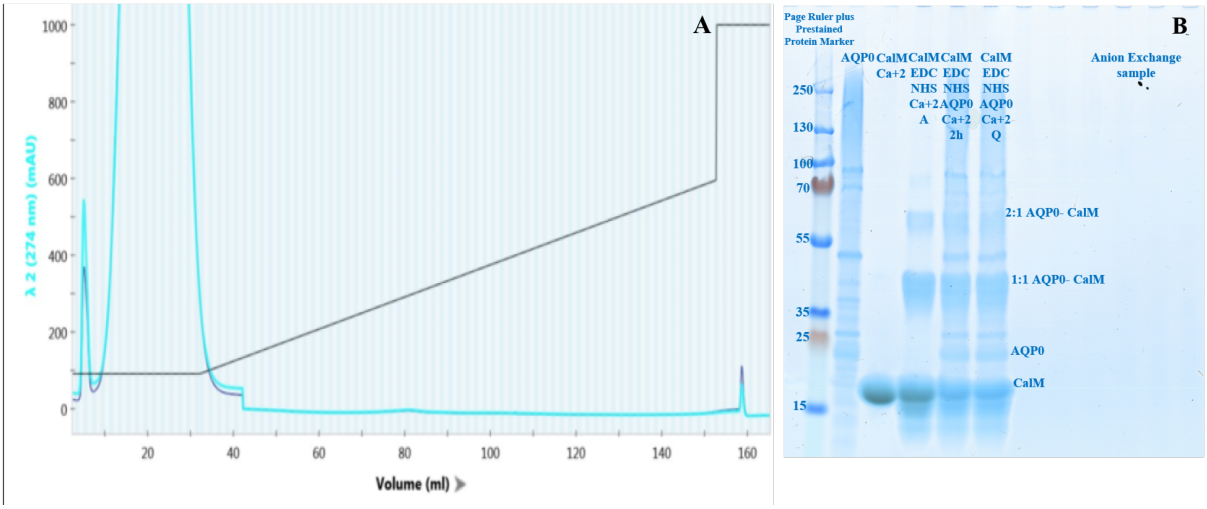

Figure 11: Anion exchange chromatogram profile (A) and SDS-PAGE gel (B). The first lane shows the multi-colour Spectra marker. The second, third and fourth lanes present the AQP0, CaM in Ca^{2+} and activated CaM with EDC and NHS, respectively. While the fifth lane corresponds to incubation of activated CaM with AQP0 for 2 h and the sixth lane is the quench reaction of AQP0-Ca^{2+} /CaM. The rest lanes represent the sample of anion exchange purification (due to experimental errors no bands were observed).

EDS-NHS cross-linker was also used to covalently cross-link the carboxyl group to amine group of a mixture of full-length AQP0-CaM and C-terminus AQP0 peptide-CaM for 30 min at room temperature. The samples were analyzed using SDS-PAGE and the results are presented in Figure 12. The SDS-PAGE analysis shows formation of the possible complex of 1:1 full-length AQP0-CaM around 45 kDa. Furthermore, SDS-PAGE shows the formation of a complex of 1:1 and 2:1 of C-terminus AQP0-CaM with approximately 18 kDa and 20 kDa, respectively.

The interactions between AQP0 and CaM were further investigated using different cross linker. BS3 covalently linked the lysine residues in a mixture of full-length AQP0-CaM and C-terminus AQP0-CaM and analyzed on SDS-PAGE as shown in Figure 12. The SDS-PAGE analysis observed possible complex formation around 45 kDa of full-length AQP0: CaM. In addition, SDS-PAGE demonstrated a complex formation of approximately 18 kDa and 20 kDa of 1:1 and 2:1 C-terminus AQP0-CaM, respectively.

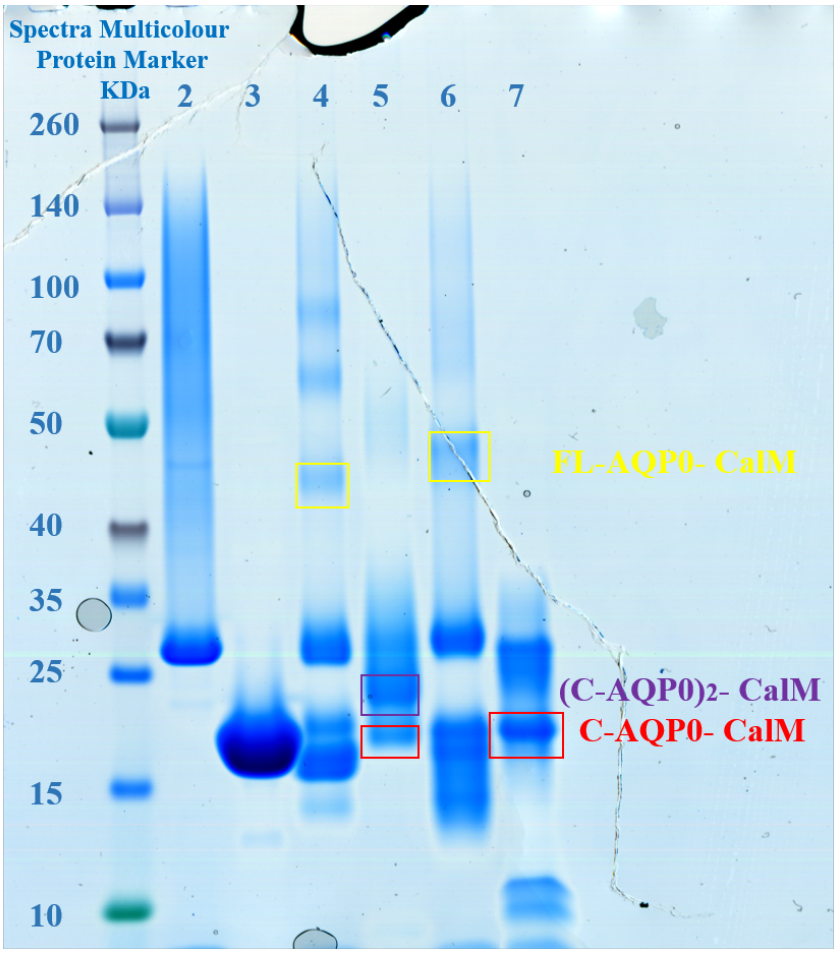

Figure 12: SDS-PAGE of an individual cross-linking experiment. One by using BS3 cross-linker and the other by using EDC-NHS cross-linker. First Lane shows the multi-colour Spectra marker. Lane 2 and 3 observe AQP0 and CaM as control, respectively. Lane 4 and 5 refer to an individual cross-linking reaction of incubation a mixture of full-length AQP0- CaM and C-terminus AQP0 - CaM with a BS3 crosslinker for 30 min at room temperature, respectively. Lane 6 and 7 representing the cross-linking reaction of incubation individually a mixture of full-length AQP- CaM and C-terminus AQP0-CaM with EDC/ NHS cross-linker for 30 min at room temperature, respectively. A possible formation complexes are shown in yellow, red and purple boxes.

As a conclusion, the results of characterization of full-length AQP0-CaM complex show that the complex is mediated by Ca^{2+} ion. In addition, the recent SDS-PAGE gel analysis showed the complex formation between the C-terminus AQP0 peptide and CaM, which is prominent and can be easily determined on the gel.

3.3.2 Cross-linking experiment of AQP2 and LIP5

In order to form the complex of AQP2 and LIP5, the first cross-linking experiment was performed at two different conditions; one by activating AQP2 and the second by activation LIP5 soluble protein. The resulted samples were purified by gel filtration and together with cross-linked sample analyzed using SDS-PAGE. Figure 13A shows that there is no complex formation during the cross-linked sample and gel filtration. To investigate the result of cross-linking reaction, a Western blot was performed using an antibody against His-tag AQP2 and LIP5 as shown in Figures 13B and 13C, respectively. The results show a formation of the possible complex around 70 kDa of 1:1 AQP2 - LIP5 when activating of AQP2.

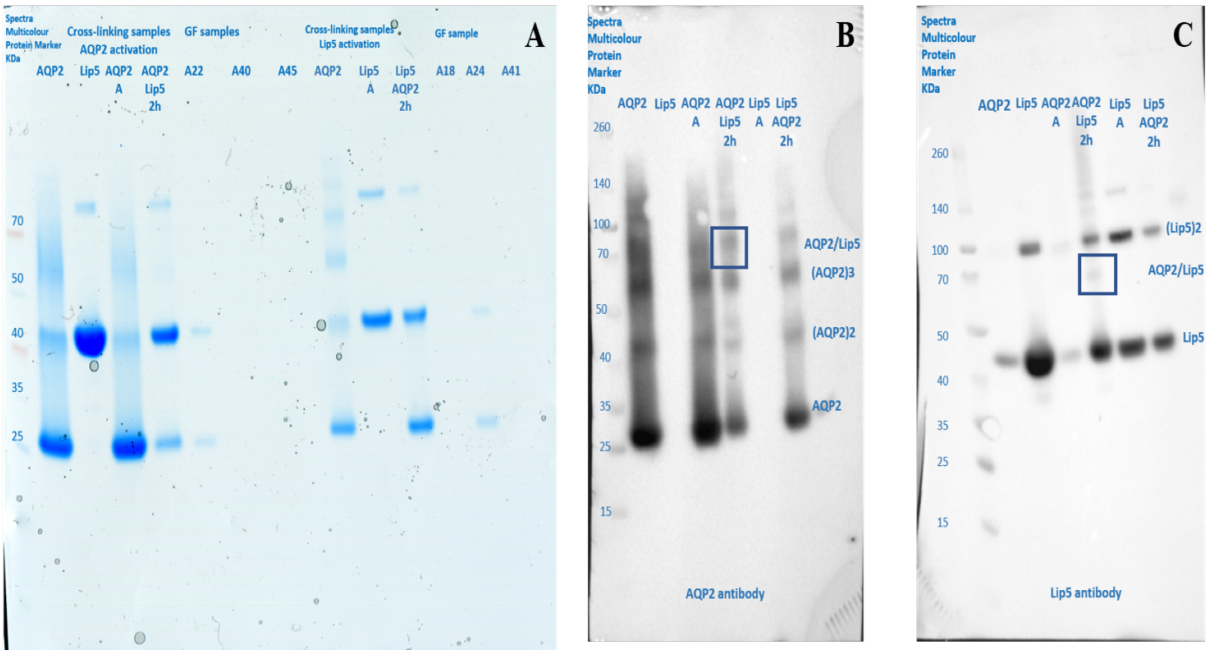

Figure 13: Cross- linked experiment of AQP2. (A) shows the duplication of the cross-linked sample analysis on SDS-PAGE gel; the first lane illustrates the mulit-colour Spectra protein marker. Lane two and three represent AQP2 and LIP5 as a control, respectively. Lane four corresponds to the activation of AQP2 with EDC: NHS for 15 min at room temperature. Lane five shows the cross-linking reaction of AQP2 with LIP5 at room temperature for 2 h. Lanes six, seven and eight correspond to the fraction of gel filtration (A22- A40 and A45) that appear clear and without any bands formation. Lane nine to fourteen are the same as pervious described sample with only one difference is that the cross-linking reaction was performed by activating LIP5 first.

(B) shows the western blot using 6 X His-tag antibodies against AQP2 and **(C)** illustrates the western blot using LIP5 antibody. Sample order on Western blot was the same in both **B and C.** Lane one shows the multi-colour Spectra protein marker while lane 2 and 3 correspond to the AQP2 and LIP5 as a control, respectively. Lane 4 observes the AQP2 activation with EDC and NHS for 15 min while lane 5 corresponds to the cross-linking reaction of AQP2 with LIP5 for 2 h at room temperature. Lane six

refers to LIP5 activation with EDC: NHS for 15 min at room temperature. Lane seven corresponds to the cross-linking reaction of LIP5 with AQP2 for 2 h at room temperature. Blue boxes in Figures B and C show the formation of possible complex when activating AQP2 first.

To obtain a high yield of the complex, another cross-linking reaction was performed using different order of sample preparation: the first one was by activating AQP2 with EDC: NHS and incubated with LIP5 for 2 h and the second one was by mixing AQP2 and LIP5, then incubated with EDC: NHS for 2 h. The outcome is illustrated using SDS-PAGE and two of Western blot using AQP2 and LIP5 antibodies, Figure 14 A, B and C.

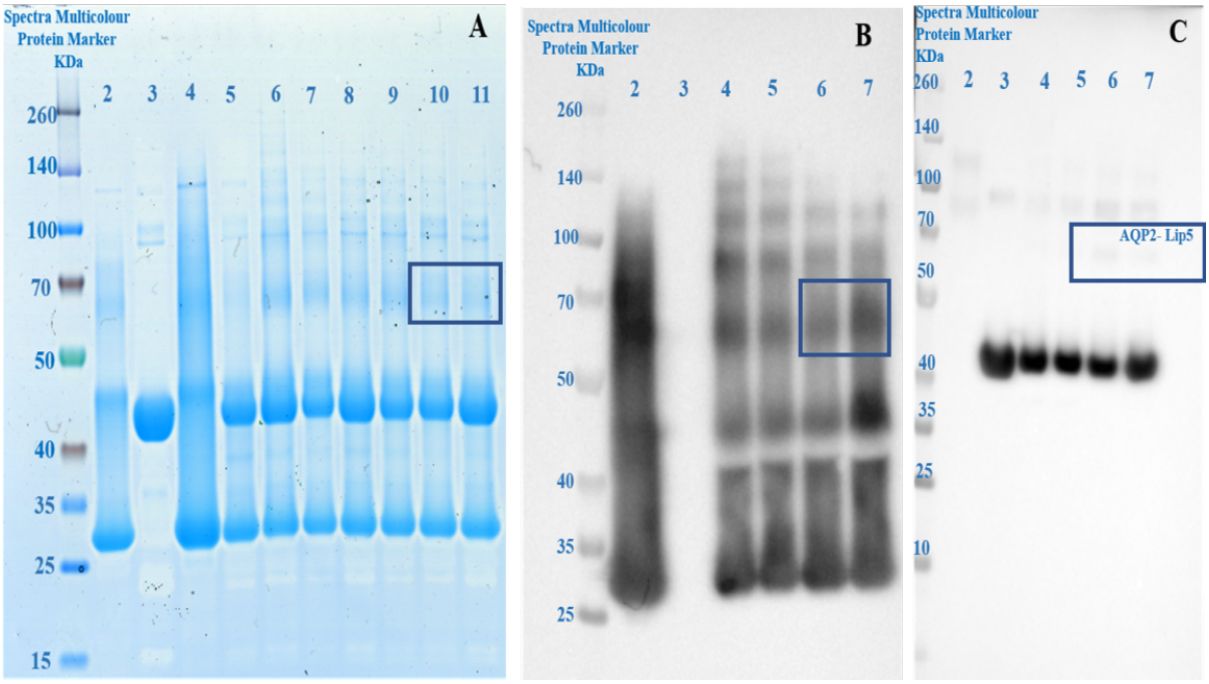

Figure 14: Cross-linking reaction of AQP2 at different order of sample preparation. (A) refers to SDS-PAGE gel; lane 1 observes protein marker. Lane 2 and 3 refer to the AQP2 and LIP5 as control, respectively. Lane 4 corresponds to the AQP2 activated with EDC and NHS. Lane 5 shows a mixture of AQP2 with LIP5. Lane 6 shows the cross-linking reaction of activated AQP2 with LIP5 at 0 h (the moment of starting cross-linking reaction). Lane 7 corresponds to the cross-linking reaction of the mixture of AQP2: LIP5 with EDC: NHS at 0h (the moment of starting cross-linking reaction). Lane 8 and 9 correspond to cross linked reaction of 6 and 7 at 1 h, respectively. Lane 10 and 11 show the cross-linked reaction of 6 and 7 at 2 h.

(B) shows the western blot using 6 X His-tag antibodies against AQP2 and **(C)** illustrates the western blot using LIP5 antibody. Sample order on Western blot was the same in both **B and C.** Lane 1, 2 and 3 refer to protein marker, AQP2 and LIP5, respectively. Lane 4 shows cross-linking reaction of incubating activated AQP2 with LIP5 at the moment of starting cross-linking reaction. Lane 5

corresponds to the cross-linking reaction of incubating the mixture of AQP2-LIP5 with EDC: NHS at the moment of starting cross-linking reaction. Lane 6 and 7 correspond to the same reaction as 4 and 5 with the only difference is the 2 h incubation. Blue boxes in Figures A, B and C show the formation of possible complex of LIP5-AQP2.

The results of performing the cross-linking reaction at different sampling order demonstrated again the possibility of formatting a complex of 1:1 of AQP2-LIP5 around 70 kDa in both situations. But again, with a weak band on the SDS-PAGE gel and both of Western blot.

In order to improve the yield of the complex, another attempt was done by performing the reaction at three different molar ratios of cross-linker of AQP2: EDC: NHS; 1:10:25, 1:8:20 and 1:6:15. Figure 15 A illustrates that there is no complex formation, which was also confirmed by Western blots using both AQP2 and LIP5 antibodies, Figure 15 B and C.

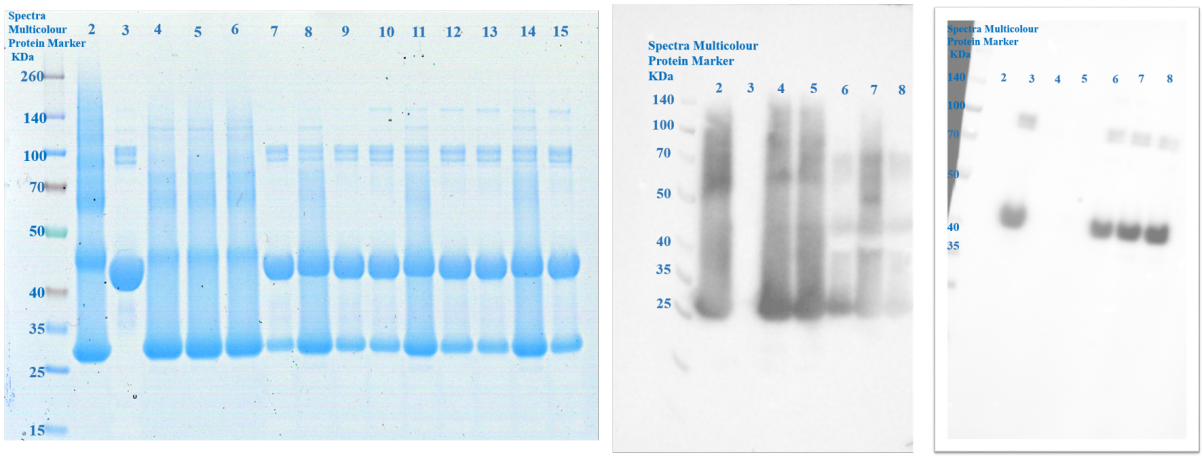

Figure 15: Cross-linking analysis of AQP2 at three different cross-linker ratios. (A) shows SDS-PAGE gel analysis; lane 1, 2 and 3 show Spectra protein marker, AQP2 and LIP5, respectively. Lane 4, 5 and 6 correspond to the AQP2 activation with EDC: NHS at 1:20:25, 1:8:20 and 1:6:15 ratio of AQP2: EDC: NHS, respectively. Lane 7, 8 and 9 correspond to the cross-linking reaction of incubating activated AQP2 with LIP5 at 0 h (at the moment of starting cross-linking reaction) with the same previous ratio, respectively. The reaction in 10, 11, 12 and 13, 14, 15 are the same as in 4,5 and 6 with only different is incubation at 1 h and 2 h, respectively.
(B) shows the western blot using 6 X His-tag antibodies against AQP2 and **(C)** illustrates the western blot using LIP5 antibody. Sample order on Western blot was the same in both **B and C.**
Lane 1, 2 and 3 show spectra protein marker, AQP2 and LIP5, respectively. Lane 4 and 5 present activations of AQP2 with EDC-NHS at 1:10:25 and 1:8:20 of AQP2: EDC: NHS ratio, respectively. Lane 6, 7 and 8 observe the cross-linking reaction of activated AQP2 with LIP5 for 2 h at 1:20:25, 1:8:20 and 1:6:15 ratio of AQP2: EDC: NHS, respectively.

A combination of all resulted of characterization of AQP2-LIP5 observed formation of possible complex around 70 kDa on SDS-PAGE, which was furthermore confirmed by Western blot.

3.3 Crystallization

Two commercial screens for crystallization of a mixture of C-terminus AQP0 peptide- CaM were set and the wells that showed initial hits after 14 days are shown below (Figure 16). The result observed precipitation and crystal formation using 2:1 C-terminus AQP0 peptide plus CaM.

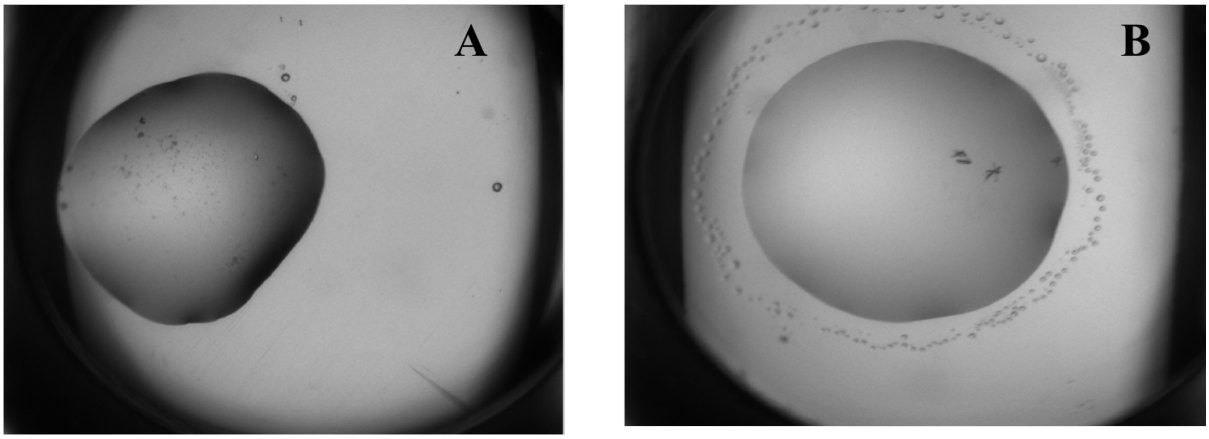

Figure 16: Co-crystallization of AQP0 C-terminal peptide and CaM. (A) drop 1 after 14 days using PACT primer screen at 20° C of 2:1 C-terminus AQP0 plus CaM using (0.2 M sodium acetate, 20 (w/v) polyethylene glycrol). **(B)** drop 2 after 14 days using JCSG- Plus at 20° C of 2:1 C-terminus AQP0 plus CaM using (0.2 M ammonium dihydrogen phosphate, 0.1 M Tris pH 8.5, 50 (v/v) 2-methy l-2,4- pentanediol).

4. Discussion

4.1-Characterizing full-length AQP0- CaM complex

Characterization of the complex between full-length AQP0 and CaM was done on basis of the previously published results using highly purified bio-reagents.

In this recent study, AQP0 was found to interact with CaM in non-canonical fashion [24]. In addition, calmodulin interacted simultaneously with two monomers of the C- terminus of AQP0 to resulted with 2:1 of CaM: AQP0 tetramer stoichiometry[24]. The complex was obtained using chemical cross-linking and analyzed by Electron microscopy [24].

In our study, repeating the chemical cross-linking experiment above did not show the formation of the complex of full-length AQP0- CaM (Figure 9 A and B). The result was unexpected in comparison to previously published results, which confirmed the formation of the full-length AQP0-CaM complex using Silver-stained SDS- PAGE and size- exclusion chromatography.

To further investigate this result, cross-linking experiment was repeated using 5 mM Ca^{2+} ion during the activation of CaM protein with EDC-NHS cross-linker. The result (Figure 10A) shows the formation of the complex of full-length AQP0- Ca^{2+}- CaM at two different ratios 1:1 and 2:1 of AQP0: Ca^{2+} /CaM around 40 kDa and 60kDa, respectively, using SDS-PAGE. To confirm the result, a Western blot was used to show the complex formation of full-length AQP0- Ca^{2+} /CaM by using a 6X His-tag antibody against C-terminus of AQP0.

The Western blot confirmed the result of SDS- PAGE gel analysis that full-length AQP0 binds to CaM in two different ratios (Figure 10 B) in presence of $Ca^{2+.}$ This result was in line with previous results in which the complex of full-length AQP0-CaM is mediated by Ca^{2+} ion. This is because the Ca^{2+} ion induced conformational change in CaM protein resulted in a transition from "closed" to "open" N- and C- termini conformational domain. This transition state leads to exposes the hydrophobic pocket of CaM and serves as a binding site to target AQP0.

The previous complex of full-length AQP0- Ca^{2+} /CaM was purified on anion exchange chromatography and analyzed on the SDS-PAGE gel (Figure 11 A and B). The chromatogram elution profile shows elution of a peak around 160 mL which was not observed on SDS-PAGE gel due to the taken the wrong sample from the plate. However, the cross-linking experiment that successfully obtained the complex of full-length AQP0-CaM was repeated several times (result not shown) with no complex formation observed. A possible reason is a large distance between carboxylic reactive groups linked to EDC/NHS of CaM and amine groups of AQP0 which cannot be linked by EDC/NHS cross-linker since they only linked carboxyl group to amine group with zero distance.

In addition, cross-linking experiment using either BS3 or EDC/NHS cross-linker were used to link a mixture of full-length AQP0- Ca^{2+} /CaM and C-terminus AQP0- Ca^{2+} /CaM (Figure12). The results show the formation of a possible complex by either using BS3 or EDC/NHS cross-linker for both the full-length AQP0 and the C-terminal AQP0 peptide.

The complex formation between the AQP0 peptide and Ca^{2+} /CaM is prominent can be easily determined on the gel. This could be due to the fact that the C- terminus AQP0 consisting of the binding site gets cross-linked easily when compared to the full-length AQP0 which is flexible thereby making the crosslinking difficult.

In summary of AQP0- CaM complex, the result demonstrates that Ca^{2+} ion is critical for the binding of CaM to AQP0 which is in line with previously reported result [25]. Further detail of characterization this complex will be continued by mass spectrometry and crystallization.

Furthermore, an attempt to characterize a mixture of C-terminus AQP0 –CaM was made using crystallization. Preliminary crystals were observed in the crystallization drops (Figure 16) that needs to be further analysed.

4.2-Producing AQP2- LIP5 complex

What is known so far is that LIP5 protein binds to the C-terminus of phosphorylated AQP2 and facilitates the lysosomal degradation of AQP2 [40]. More specifically, LIP5 binds region L230 to D243 of AQP2 and this binding is dependent of AQP2 phosphorylation (at Ser256). However, complex characterization and the mechanisms of binding of phosphorylated AQP2-LIP5 still remains unclear and need to be established. In this study, chemical cross-linking optimization using highly purified bio-reagents was used to obtain the complex of AQP2 and LIP5. Chemical cross-linking of AQP2 to LIP5 showed a formation of possible complex around 70 kDa during activating AQP2 first Figure 13 B and C on Western blot. The reason for this might be probably due to the full-length AQP2 is rich in carboxyl group more than the LIP5.

Therefore, to obtain a high yield of the potential complex at 70 kDa, another cross-linking experiment was performed. The result on SDS- PAGE gel and two of Western blot using antibodies against AQP2 and LIP5 observed the formation of the complex of the previse result but again with very low yield Figure 14 A, B and C.

Furthermore, the cross-linking experiment was repeated once again using different molar ratios of the cross-linker Figure 15 A, B and C. The resulted showed no complex formation. The reason for that could be the long distance between the carboxyl group to amino group which cannot be served using EDC- NHS since they only attached carboxyl of the first protein to an

amine group of second protein with zero distance. However, for future work, binding interactions study of full-length AQP0- CaM and C-terminus AQP- CaM by cross-linking experiment could be continued and be analysed using mass spectrometry and crystallization. Furthermore, interaction between AQP2 and LIP5 could be tested using different cross-linker.

Conclusion

I demonstrated the ability to use chemical cross-linking experiment to obtain complexes between membrane proteins and regulatory proteins, specifically the complexes between AQP0 and CaM and AQP2 and LIP5.

Acknowledgement

I take this opportunity to express my sincere thanks to my supervisor Dr. Susanna Törnroth-Horsefield for unwavering support, guidance and insight through this research project. I also thank my lab supervisor Veronika Nesverova, Jennifer Virginia Roche and Stefan Kreida for their help and support. I extend my thanks to my husband and parents for unceasing encouragement, support and attention.

References

1. Agre P, Preston GM, Smith BL, Jung JS, Raina S, Moon C, Guggino WB, Nielsen S: **Aquaporin Chip - the Archetypal Molecular Water Channel**. *Am J Physiol* 1993, **265**(4):F463-F476.
2. Agre P: **The Aquaporin Water Channels**. *Proceedings of the American Thoracic Society* 2006, **3**(1):5-13.
3. Chaumont F, Barrieu F, Wojcik E, Chrispeels MJ, Jung R: **Aquaporins constitute a large and highly divergent protein family in maize**. *Plant Physiol* 2001, **125**(3):1206-1215.
4. Hashido M, Kidera A, Ikeguchi M: **Water transport in aquaporins: osmotic permeability matrix analysis of molecular dynamics simulations**. *Biophys J* 2007, **93**(2):373-385.
5. Verkman AS: **Aquaporins in Clinical Medicine**. *Annu Rev Med* 2012, **63**:303-316.
6. Ishibashi K, Hara S, Kondo S: **Aquaporin water channels in mammals**. *Clin Exp Nephrol* 2009, **13**(2):107-117.
7. Bjorkskov FB, Krabbe SL, Nurup CN, Missel JW, Spulber M, Bomholt J, Molbaek K, Helix-Nielsen C, Gotfryd K, Gourdon P *et al*: **Purification and functional comparison of nine human Aquaporins produced in Saccharomyces cerevisiae for the purpose of biophysical characterization**. *Sci Rep* 2017, **7**(1):16899.
8. Walz T, Fujiyoshi Y, Engel A: **The AQP structure and functional implications**. *Handb Exp Pharmacol* 2009(190):31-56.
9. Fields JB, Nemeth-Cahalan KL, Freites JA, Vorontsova I, Hall JE, Tobias DJ: **Calmodulin Gates Aquaporin 0 Permeability through a Positively Charged Cytoplasmic Loop**. *J Biol Chem* 2017, **292**(1):185-+.
10. Rose KML, Wang Z, Magrath GN, Hazard ES, Hildebrandt JD, Schey KL: **Aquaporin 0 calmodulin interaction and the effect of Aquaporin 0 phosphorylation**. *Biochemistry-Us* 2008, **47**(1):339-347.
11. Chepelinsky AB: **The ocular lens fiber membrane specific protein MIP/aquaporin 0**. *J Exp Zool Part A* 2003, **300a**(1):41-46.
12. Roche JV, Tornroth-Horsefield S: **Aquaporin Protein-Protein Interactions**. *Int J Mol Sci* 2017, **18**(11).
13. Gonen T, Cheng Y, Kistler J, Walz T: **Aquaporin-0 membrane junctions form upon proteolytic cleavage**. *J Mol Biol* 2004, **342**(4):1337-1345.
14. Nemeth-Cahalan KL, Kalman K, Hall JE: **Molecular basis of pH and Ca2+ regulation of aquaporin water permeability**. *J Gen Physiol* 2004, **123**(5):573-580.
15. Ball LE, Little M, Nowak MW, Garland DL, Crouch RK, Schey KL: **Water permeability of C-terminally truncated aquaporin 0 (AQP0 1-243) observed in the aging human lens**. *Invest Ophthalmol Vis Sci* 2003, **44**(11):4820-4828.
16. Varadaraj K, Kumari S, Shiels A, Mathias RT: **Regulation of aquaporin water permeability in the lens**. *Invest Ophthalmol Vis Sci* 2005, **46**(4):1393-1402.
17. Reichow SL, Gonen T: **Noncanonical binding of calmodulin to aquaporin-0: implications for channel regulation**. *Structure* 2008, **16**(9):1389-1398.
18. Sasagawa T, Ericsson LH, Walsh KA, Schreiber WE, Fischer EH, Titani K: **Complete amino acid sequence of human brain calmodulin**. *Biochemistry-Us* 1982, **21**(10):2565-2569.
19. Chattopadhyaya R, Meador WE, Means AR, Quiocho FA: **Calmodulin structure refined at 1.7 Å resolution**. *J Mol Biol* 1992, **228**(4):1177-1192.
20. Walsh MP: **Calmodulin and its roles in skeletal muscle function**. *Can Anaesth Soc J* 1983, **30**(4):390-398.
21. Baba ML, Goodman M, Berger-Cohn J, Demaille JG, Matsuda G: **The early adaptive evolution of calmodulin**. *Mol Biol Evol* 1984, **1**(6):442-455.
22. Finn BE, Evenas J, Drakenberg T, Waltho JP, Thulin E, Forsen S: **Calcium-induced structural changes and domain autonomy in calmodulin**. *Nat Struct Biol* 1995, **2**(9):777-783.
23. Ogawa Y, Tanokura M: **Calcium binding to calmodulin: effects of ionic strength, Mg2+, pH and temperature**. *J Biochem* 1984, **95**(1):19-28.

24. Reichow SL, Clemens DM, Freites JA, Nemeth-Cahalan KL, Heyden M, Tobias DJ, Hall JE, Gonen T: **Allosteric mechanism of water-channel gating by Ca2+-calmodulin**. *Nat Struct Mol Biol* 2013, **20**(9):1085-1092.
25. Zhang XY, Wang B, Guan YF: **Nuclear Receptor Regulation of Aquaporin-2 in the Kidney**. *Int J Mol Sci* 2016, **17**(7).
26. Kwon TH, Frokiaer J, Nielsen S: **Regulation of aquaporin-2 in the kidney: A molecular mechanism of body-water homeostasis**. *Kidney Res Clin Pract* 2013, **32**(3):96-102.
27. van Balkom BW, Boone M, Hendriks G, Kamsteeg EJ, Robben JH, Stronks HC, van der Voorde A, van Herp F, van der Sluijs P, Deen PM: **LIP5 interacts with aquaporin 2 and facilitates its lysosomal degradation**. *J Am Soc Nephrol* 2009, **20**(5):990-1001.
28. Pearce D, Soundararajan R, Trimpert C, Kashlan OB, Deen PMT, Kohan DE: **Collecting Duct Principal Cell Transport Processes and Their Regulation**. *Clin J Am Soc Nephro* 2015, **10**(1):135-146.
29. van Balkom BW, Savelkoul PJ, Markovich D, Hofman E, Nielsen S, van der Sluijs P, Deen PM: **The role of putative phosphorylation sites in the targeting and shuttling of the aquaporin-2 water channel**. *J Biol Chem* 2002, **277**(44):41473-41479.
30. McDill BW, Li SZ, Kovach PA, Ding L, Chen F: **Congenital progressive hydronephrosis (cph) is caused by an S256L mutation in aquaporin-2 that affects its phosphorylation and apical membrane accumulation**. *Proc Natl Acad Sci U S A* 2006, **103**(18):6952-6957.
31. Tamma G, Robben JH, Trimpert C, Boone M, Deen PM: **Regulation of AQP2 localization by S256 and S261 phosphorylation and ubiquitination**. *Am J Physiol Cell Physiol* 2011, **300**(3):C636-646.
32. Kamsteeg EJ, Hendriks G, Boone M, Konings IB, Oorschot V, van der Sluijs P, Klumperman J, Deen PM: **Short-chain ubiquitination mediates the regulated endocytosis of the aquaporin-2 water channel**. *Proc Natl Acad Sci U S A* 2006, **103**(48):18344-18349.
33. Lee YJ, Lee JE, Choi HJ, Lim JS, Jung HJ, Baek MC, Frokiaer J, Nielsen S, Kwon TH: **E3 ubiquitin-protein ligases in rat kidney collecting duct: response to vasopressin stimulation and withdrawal**. *Am J Physiol Renal Physiol* 2011, **301**(4):F883-896.
34. Ward DM, Vaughn MB, Shiflett SL, White PL, Pollock AL, Hill J, Schnegelberger R, Sundquist WI, Kaplan J: **The role of LIP5 and CHMP5 in multivesicular body formation and HIV-1 budding in mammalian cells**. *J Biol Chem* 2005, **280**(11):10548-10555.
35. Boone M, Mobasheri A, Fenton RA, van Balkom BWM, Wismans R, van der Zee CEEM, Deen PMT: **The lysosomal trafficking regulator interacting protein-5 localizes mainly in epithelial cells**. *J Mol Histol* 2010, **41**(1):61-74.
36. Piper RC, Katzmann DJ: **Biogenesis and function of multivesicular bodies**. *Annu Rev Cell Dev Biol* 2007, **23**:519-547.
37. Babst M: **MVB vesicle formation: ESCRT-dependent, ESCRT-independent and everything in between**. *Curr Opin Cell Biol* 2011, **23**(4):452-457.
38. Azmi I, Davies B, Dimaano C, Payne J, Eckert D, Babst M, Katzmann DJ: **Recycling of ESCRTs by the AAA-ATPase Vps4 is regulated by a conserved VSL region in Vta1**. *The Journal of Cell Biology* 2006, **172**(5):705-717.
39. Scott A, Chung HY, Gonciarz-Swiatek M, Hill GC, Whitby FG, Gaspar J, Holton JM, Viswanathan R, Ghaffarian S, Hill CP *et al*: **Structural and mechanistic studies of VPS4 proteins**. *Embo J* 2005, **24**(20):3658-3669.
40. Roche JV, Survery S, Kreida S, Nesverova V, Ampah-Korsah H, Gourdon M, Deen PMT, Tornroth-Horsefield S: **Phosphorylation of human aquaporin 2 (AQP2) allosterically controls its interaction with the lysosomal trafficking protein LIP5**. *J Biol Chem* 2017, **292**(35):14636-14648.